# MODIFICATION OF A MODEL REDUCTION ALGORITHM FOR SWITCHED DYNAMIC MODELS: SYNCHRONOUS GENERATOR CASE

Israel Núñez-Hernández
Robotics and Mechatronics Group
University of Twente
Enschede, The Netherlands
E-mail: i.nunezhernandez@utwente.nl

Peter C. Breedveld
Robotics and Mechatronics Group
University of Twente
Enschede, The Netherlands
E-mail: P.C.Breedveld@utwente.nl

Paul B. T. Weustink
Controllab Products B.V
Hengelosestraat 500, 7521AN
Enschede, The Netherlands
E-mail: paul.weustink@controllab.nl

**KEYWORDS**
Model order reduction algorithm, activity, synchronous generator, bond graph, hardware-in-the-loop simulation, energy.

**ABSTRACT**

An energy-based model reduction technique is discussed and modified in order to make it applicable to models that suddenly switch from one type of behavior to another. The method and its modification are applied to an example of a synchronous generator under open- and short-circuit tests. The successfully reduced model can be used for Hardware-In-the-Loop (HIL) simulation of the control system.

## INTRODUCTION

A Hardware-In-the-Loop system (Hanselmann,1996) and (Ledin, 1999) connects a real-time simulation model with physical components operating in the real world, most commonly a controller. Real-time simulation models face several challenges; principally they must obtain a good accuracy while using relatively simple, fixed-step integration methods. The complexity of current simulation models has resulted in a contradistinction for engineers that need real-time solutions: larger and more complex models imply that more differential equations need to be solved in a fixed-time. This paper seeks to remedy this problem by reducing the model order by means of an energetic analysis of the system. A model of a synchronous generator is taken as an example. Firstly, it is required to model the system in such a manner that the power exchange is explicitly shown. The (power) port-based approach, represented by bond graphs, is chosen, given its explicit description of power and energy and built-in compliance with the energy conservation principle. Secondly, the model order reduction is achieved by the application of an algorithm already developed by Louca et al. (1997). This algorithm weighs the so-called activity (an energy-based metric) of the elements in a bond graph model, and it reduces the model by removing the least active elements. However, the original algorithm has a limitation when the system contains switches. Therefore, an algorithm modification is proposed.
This paper has been organized in the following way. In section 2 an overview of the bond graph notation is given. The model order reduction by Louca et al (1997) based on energy and its corresponding algorithm is discussed in Section 3. In section 4, a brief description of a classical model of the synchronous generator is given. The bond graph model is obtained next from the equivalent electrical circuit and extended with the mechanical part of the model. This model is used to generate simulation results. In section 5 a modification of the model order reduction algorithm is proposed and simulation results are shown. Finally, conclusions and plans for future work are stated.

## BOND GRAPHS

The port-based approach with regard to modeling of physical systems is an effective way to split a system into conceptual elements that are interacting with each other via (power) ports. As it is based on energy, port-based modelling offers a unified way to model physical systems from different physical domains, such as electrical, magnetic, mechanical, hydraulic, thermal, etc.
A bond graph (BG) is a graphical notation of such a port-based description. The BG conceptual framework was originated by Paynter (1961). This graphical technique is based on representing power transfer between elements as labelled nodes, which are linked to each other by means of oriented edges called *bonds*. In each physical domain, the power can be written as the product of two variables, *effort* $e(t)$ and *flow* $f(t)$. This pair of variables is called *power variables*. In a BG, the way in which these variables need to be computed in a dynamic model is indicated by means of a so-called *causal stroke*. It is a perpendicular line put at one end of a bond indicating the computational direction of the effort signal, also called the *causality*.
The port-based approach is in principle an object-oriented approach to modeling. This permits different realizations of an object by directly removing and/or replacing a portion of it with another BG system with a different degree of dynamic details. The basic elements (nodes) of the BG language can be classified as follows

- 1-port elements, which dissipate (free) energy (resistor $R$), store energy (inertia $I$, capacitor $C$) and supply power (sources $S_e$, $S_f$).
- 2-port elements (transformers $TF$ and gyrators $GY$) are used when it is necessary to scaling variables (transformer) or interconnect submodels in different domains in a power conservative way.
- Multiport elements that represent the conceptual structure of the model. The 0-*junction* is a BG node

Proceedings 29th European Conference on Modelling and Simulation ©ECMS Valeri M. Mladenov, Petia Georgieva, Grisha Spasov, Galidiya Petrova (Editors)
ISBN: 978-0-9932440-0-1 / ISBN: 978-0-9932440-1-8 (CD)

with common effort; the 1-*junction* describes a common flow node.

If the reader is interested in more details about BG, you may refer to Karnopp et al. (1990), and Borutzky (2010).

## MODEL ORDER REDUCTION

Model reduction is aimed at decreasing the complexity of a model to achieve a balance between accuracy and computational efficiency. As physical processes are considered that are assumed to obey the basic principles of physics where energy conservation is a leading principle, it is reasonable to propose a metric based on energy.

This paper will focus on an energy-based metric, called *activity* proposed by Louca et al. (1997). Activity provides an indication of energy that flows through or is exchanged in each element over a particular time span. Activity is the integral of absolute value of power flow of a 1-port element (i.e. *R*, *C*, or *I* elements):

$$A = \int_{\tau_1}^{\tau_2} \left| P(t) \right| dt = \int_{\tau_1}^{\tau_2} \left| e(t) f(t) \right| dt \qquad (1)$$

where $P(t)$ is the instantaneous power at the energy element, and $[\tau_1,\tau_2]$ is the time window for which the model has to predict the system behavior.

Activity has units of energy. Nevertheless, energy and activity are different because of the absolute value in activity definition. The utility of activity lies in its direct application on linear and non-linear systems. It is necessary to obtain the *total activity* on the system, and is defined as

$$A^{total} = \sum_{i=1}^{k} A_i \qquad (2)$$

where $A_i$ is the activity of the *i*-th element as defined in Equation (1). Finally, it is possible to calculate a normalized measure of element importance, this quantity is called *activity index*, *AI*, and is given by

$$AI_i = 100\left( A_i / A^{total} \right) \qquad (3)$$

Thus, an element with low activity index has a negligible contribution to the total system activity, and therefore, it may be eliminated from the model.

As mentioned before, the topological description of energy in a dynamic system by means of a BG are in particular compatible with this activity metric. For example, the elimination of low activity elements is easily done in a BG model by simply removing these elements.

### Algorithm

The Model Order Reduction Algorithm (MORA) is proposed by Louca et al. (1997). The global structure of MORA is shown in Figure 1.

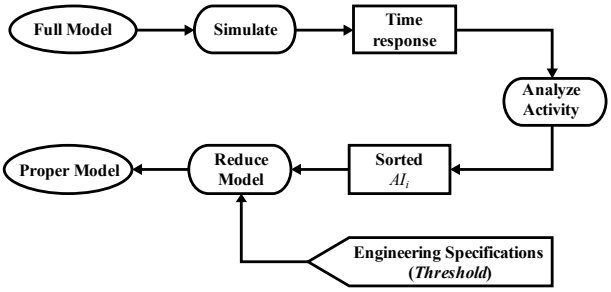


Figure 1: Model Order Reduction Algorithm

MORA considers the reduction of a given "full model", i.e. the model to be reduced. Firstly, the activity of each energy element is calculated. Secondly, the total activity, and the activity index are calculated. Then, the activity indices are sorted in descending order, and arranged in a vector *r*, thus

$$r = \left[ r_1 \quad \cdots \quad r_k \right]^T \equiv \left[ \text{highest } AI \quad \cdots \quad \text{lowest } AI \right]^T \qquad (4)$$

A threshold representing the activity percentage retained after reduction is given by the user.

The sorted activity indices are summed until the *cumulative activity index* (*CAI*) exceeds the threshold. The cumulative index is calculated by

$$CAI_i = CAI_{i-1} + AI_{r_i}; \quad i = 1,\ldots,k; \quad CAI_0 = 0 \qquad (5)$$

Finally, the elements accounted for the *CAI* are included in the reduced model. The remaining elements may be removed.

## SYNCHRONOUS GENERATOR

The aim of this section is to familiarize the reader with the acquisition of a BG model on the basis of a classical model of a synchronous machine.

The synchronous machine is an electromechanical energy converter composed of a rotating part named *rotor* or *field*, and a 'fixed' part (housing) named *stator* or *armature*. In the armature windings, a rotating magnetic field is generated either by injecting AC (motor) or by turning the rotor carrying a constant field (generator). As the adjective 'synchronous' suggests, the rotor rotates at the same frequency as the rotating stator magnetic field during steady-state operation.

The synchronous generator (SG) is commonly modeled by means of a transformation proposed by Park (1929). This coordinate transformation $P(\theta_r)$ changes the stator variables in a natural reference frame ($f_{abc}$) to a reference frame fixed in the rotor ($f_{dq0}$).

A salient-pole SG as shown in Figure 2 is considered, where the *d*-axis is chosen in the same direction as the field generated by the field winding *f*. Two damper windings are attached in such a way that one is in line with the *d*-axis (*D* winding), and the second (*Q* winding) is attached to the *q*-axis.

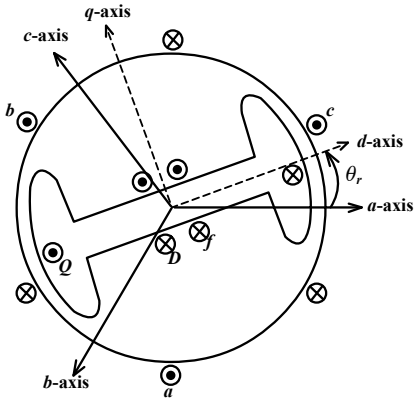

Figure 2 Salient-pole synchronous machine reference frames

In this paper, it is assumed that the *q*-axis is orthogonally leading the *d*-axis, and the rotor angle is referred to the *d*-axis, such that the Park transformation becomes:

$$\begin{bmatrix} f_d \\ f_q \\ f_0 \end{bmatrix} = \underbrace{\sqrt{\frac{2}{3}} \begin{bmatrix} \cos\theta_r & \cos(\theta_r - 2\pi/3) & \cos(\theta_r + 2\pi/3) \\ -\sin\theta_r & -\sin(\theta_r - 2\pi/3) & -\sin(\theta_r + 2\pi/3) \\ 1/\sqrt{2} & 1/\sqrt{2} & 1/\sqrt{2} \end{bmatrix}}_{P(\theta_r)} \begin{bmatrix} f_a \\ f_b \\ f_c \end{bmatrix} \tag{6}$$

where the rotor angle is $\theta_r = N_{pp} \int \omega_n \, dt$, with $N_{pp}$ equal to the number of poles-pairs in the rotor, and $\omega_n$ is the mechanical angular velocity.

It is common practice among generator manufacturers to provide the parameters in per-unit (pu) impedances rather than inductances values. Because of this, Rankin (1945) suggest to normalize the equations to a convenient base value and express all voltages in pu (or percent) of a base. The reader may refer to Anderson and Fouad (2003) for more details about the pu system.

Assuming that the positive stator current is directed outward of the terminals, and considering that for balanced three-phase systems the *0*-axis in Equation (6) is zero, and a linear magnetic system, the voltage equations in pu of the SG described in IEEE Std. 1110 (2002) may be expressed as

$$\begin{aligned} v_d &= -r_s\, i_d - \tfrac{\omega_r}{\omega_e}\lambda_q + \tfrac{1}{\omega_e}\tfrac{d}{dt}\lambda_d & v_f &= r_f\, i_f + \tfrac{1}{\omega_e}\tfrac{d}{dt}\lambda_f \\ v_q &= -r_s\, i_q + \tfrac{\omega_r}{\omega_e}\lambda_d + \tfrac{1}{\omega_e}\tfrac{d}{dt}\lambda_q & 0 &= r_D\, i_D + \tfrac{1}{\omega_e}\tfrac{d}{dt}\lambda_D \\ & & 0 &= r_Q\, i_Q + \tfrac{1}{\omega_e}\tfrac{d}{dt}\lambda_Q \end{aligned} \tag{7}$$

The magnetic flux linkage equations are defined by

$$\begin{aligned} \lambda_d &= -X_{ls}\, i_d + X_{md}(-i_d + i_f + i_D) \\ \lambda_f &= X_{lf}\, i_f + X_{md}(-i_d + i_f + i_D) \\ \lambda_D &= X_{lD}\, i_D + X_{md}(-i_d + i_f + i_D) \\ \lambda_q &= -X_{ls}\, i_q + X_{mq}(-i_q + i_Q) \\ \lambda_Q &= X_{lQ}\, i_Q + X_{mq}(-i_q + i_Q) \end{aligned} \tag{8}$$

where $\{i_D, i_Q\}$, $\{\lambda_D, \lambda_Q\}$, $\{r_D, r_Q\}$, $\{X_{lD}, X_{lQ}\}$ are the direct and quadrature dampers currents, magnetic flux linkages, resistances, and leakage reactances; $\{i_d, i_q\}$, $\{\lambda_d, \lambda_q\}$, $\{v_d, v_q\}$, $\{X_{md}, X_{mq}\}$ are the stator currents, magnetic flux linkages, voltages, and mutual reactances referred to the rotor frame; $i_f$, $v_f$, $\lambda_f$, $r_f$, $X_{lf}$ are the current, voltage, magnetic flux linkage, resistance, and leakage reactance in the field winding; $\omega_e$ is the electrical angular velocity; finally, $r_s$, $X_{ls}$ are the stator winding resistance, and leakage reactance referred to the rotor frame.

From Equations (7) and (8) can be deduced the SG equivalent circuit, Figure 3.

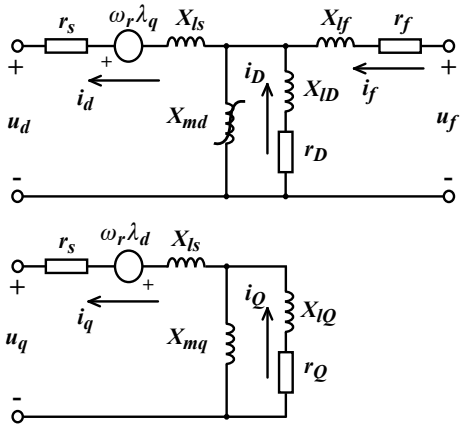

Figure 3: SG equivalent circuit on *d*-, and *q*-axis

The saturation effect is confined to the mutual inductances. It is assume that $X_{mq}$ does not saturate, simply because the *q*-axis flux is usually quite small in comparison to the *d*-axis flux due to the effect of the field winding. This assumption is sufficient for salient-pole machines but insufficient for round-rotor machines.

There are several methods to add saturation on a synchronous machine. Herein, the method described by Corzine et al. (1998) was applied.

At the other hand, the mechanical part of the SG may be model by the swing equation.

$$J \tfrac{1}{N_{pp}} \tfrac{d\omega_n}{dt} = T_m - T_e - b\,\omega_n \tag{9}$$

where $J$ is the moment of inertia of all rotating masses attached to the shaft, $T_m$ is the mechanical driving torque, $b$ is the friction coefficient. The electromagnetic torque in terms of rotor reference-frame variables is given by

$$T_e = N_{pp}\left(\lambda_d\, i_q - \lambda_q i_d\right) \tag{10}$$

**The Bond Graph Model**

The principal advantage of BG models over their equivalent circuit counterparts is that they can be directly interconnected with (sub-)models from other physical domains in a unified graphical modeling language.

Notice the modulated (or 'controlled') voltage sources shown in the electrical circuit in Figure 3. These sources, which express the electromotive forces (*emf*) induced in the stator by the rotor movement, are in fact equivalent with the electrical port of a 2-port modulated gyrator (MGY) of which the other, mechanical, port represents the power exchanged with the mechanical domain.

The advantage of BG modeling becomes relevant at this point: the electrical circuit does not show a link between the mechanical and the electrical domain. This link is described by Equation (10), where the torque is a function of two electrical variables; which completes the second side of the MGY's with gyration ratios $\lambda_d$ and $\lambda_q$. Their contributions are added according to their orientations at a 1-*junction* and weighted by a transformer (TF) with ratio $N_{pp}$ (cf. Figures 3 and 4).
The previous statements explain the two MGY linking the 1-*junctions* associated with the *d*- and *q*-stator currents and the 1-*junction* associated with rotor angular velocity, $\omega_r = N_{pp}\,\omega_n$ .

Finally, the mechanical domain is completed by using Equation (9), where a 1-*junction* represents the torque balance of the swing equation. Then, the equivalent circuit given in Figure 3 can be converted into a BG model as Sahm (1979) described, see Figure 4.
The magnetic phenomena in each axis are modeled by means of *I*-multiport storage elements described by Breedveld (1985). Each *I*-multiport incorporates the constitutive relationship between magnetic fluxes and currents, defined in Equation (8). The magnetic saturation is added in the *I*-multiport on the *d*-axis. The saturation curve was obtained from measurement specifications of the generator. In order to represent a mechanical torque, a effort source ($S_e : T_m$) is added to the mechanical domain.

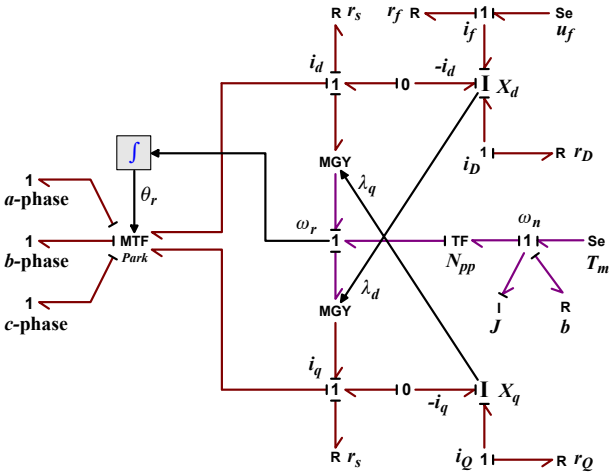

Figure 4: Synchronous generator bond graph model

## Synchronous Generator Validation

Firstly, from the generator specification datasheet (see Appendix A), and according to the IEEE Std. 1110 (2002) the necessary parameters are calculated.
Secondly, for the purpose of validation, the simulation results of an open-circuit test, and a short-circuit test are compared with the measurements data given by the manufacturer. The BG model in Figure 4 needs a modification in order to simulate the previously mentioned tests. To achieve this, a *switched 1-junction* (X1) proposed by Breedveld (1996) and Junco et al. (2007) is included in each phase; see Figure 5.

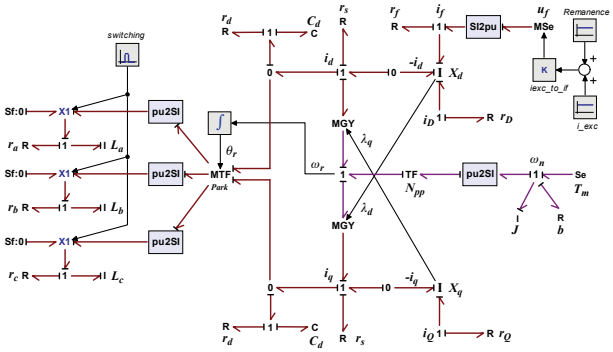

Figure 5: Sudden short-circuit test in bond graphs

The BG model shown in Figure 5 contains three zero-flow sources $S_f$:0, which represent the open-circuit state of the machine. The "pu2SI" blocks allow a conversion between the pu values at the machine and the actual values in the International System of Units (SI). The remanence effect of the machine as well as a linear relation between the generator excitation current and the exciter excitation current are modulating effect and can therefore be added at the signal level by means of a block diagram representation at the rotor side. A short-circuit test can be simulated by adding one *RL* load with very small parameter values to each phase.
Two *RC* combinations at the output of *d*- and *q*-axis represent the stray capacitive effects of the machine. Common models only contain a large resistor at this output in order to make the model computationally consistent. However, a large resistor in combination with the impedances inside the I-multiport (or the load impedance) implies high frequencies.
Figure 6 shows the steady-state voltage at *phase-a* ($u_a$) when the generator is operating in open-circuit while the field current is increased gradually.

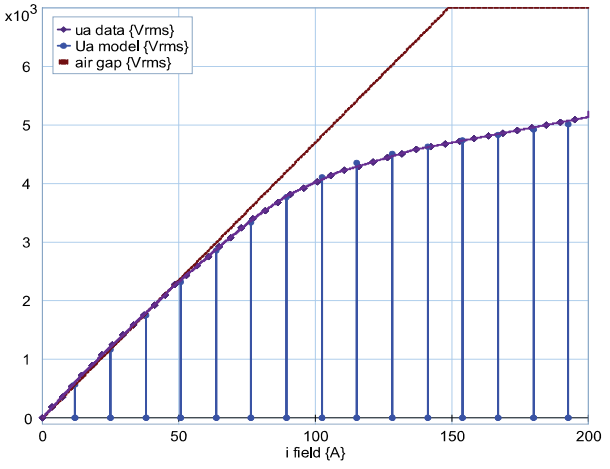

Figure 6: Open-circuit curve, simulation and data

A short-circuit test is done, Figure 7 shows the steady-state current at *phase-a* ($i_a$) as function of the field current. The simulation results obtained from 20-sim® compared with measurement data show that the model gives an accurate enough description of the machine behavior.

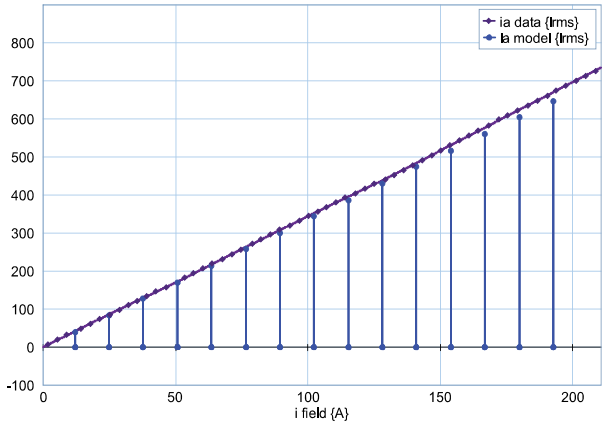

Figure 7: Short-circuit curve, simulation and data

Validation of these results will only take place after this industrially used machine becomes available for this purpose. Nevertheless, the match between measurement specification data, standard equations used to describe the dynamic behavior and the BG model herein shows that a competent model for our purpose has been obtained.

## ALGORITHM IMPLEMENTATION AND RESULTS

Once the model of the SG has been validated, a test of model reduction by means of MORA is considered in which the generator is operating in open-circuit at nominal voltage, and after 30 sec., a sudden short-circuit is done and after 65 sec., the circuit is opened again. The outputs of interest are the voltage and current at *phase-a*, torque in the shaft, and field current. Table 1 shows the activity indices as sorted by MORA. Based on a model reduction threshold, $\beta$=99.5%, MORA suggest the elimination of just one element (element shown in shadow in Table 1).

It is important to notice that, the *RC* set elements are not considered in the measured activity, since they are parasite effects and is evident that they will have low activity.

Table 1: Full test element activity indices

| Ele. | AI (%) | CAI (%) | Ele. | AI (%) | CAI (%) |
|---|---|---|---|---|---|
| $r_{sd}$ | 30.539 | 30.539 | $X_{lD}$ | 3.151 | 95.376 |
| $r_f$ | 23.029 | 53.569 | $X_{ad}$ | 1.256 | 96.631 |
| $X_{lf}$ | 19.410 | 72.978 | $X_{aq}$ | 1.251 | 97.882 |
| $X_{lsd}$ | 9.975 | 82.953 | $r_Q$ | 0.828 | 98.710 |
| $X_{lQ}$ | 5.784 | 88.737 | $r_D$ | 0.818 | 99.529 |
| $X_{lsq}$ | 3.488 | 92.225 | $r_{sq}$ | 0.471 | 100.000 |

As shown in Table 1, most of the elements cannot be neglected. The high activity due to a sudden short-circuit test represents a high load impact, and it excites the damper windings. MORA cannot distinguish the different stages of the machine produced by the switches. Thus, the need of a modification of MORA to obtain a useful model reduction is evident, this modification will be named Switched MORA (SMORA).

The proposed approach is based on time segmentation. MORA needs to be applied for different time windows according to the responses that the user wishes to maintain. The final conditions of the previous stage are considered as initial conditions in the actual stage. The SMORA procedure is shown in Figure 8.

Figure 8 shows that there will be *k*-models when the algorithm is finished. By simulating these reduced models one after the other it is possible to obtain the full behavior of the system.

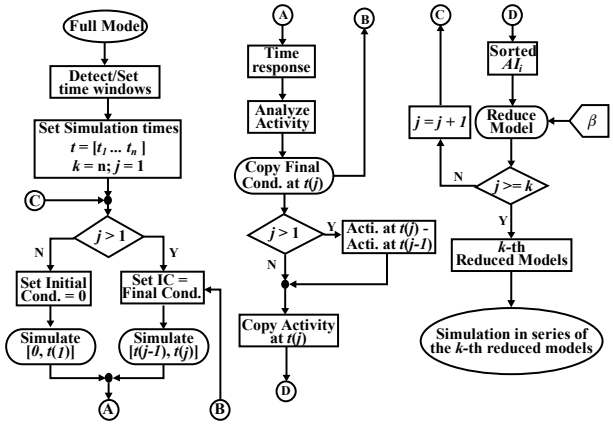

Figure 8: Diagram flow for Switched MORA (SMORA)

For a quantitative comparison, the fitness of the reduced model can be measured by using the best fit percentage (BFT) defined as follows:

$$BFT = 100\left(1 - \frac{\| w - w_r \|_2}{\| w_r - \mu_r \|_2}\right) \qquad (11)$$

where $w$ and $w_r$ are the outputs of the original and reduced model, respectively. $\|\ldots\|_2$ is the Euclidean norm, and $\mu_r$ is the mean of the reduced model output.

For the case of the generator, the time windows to be considered are characterized by the subtransient and transient time constants. They represent the time after which the effect of the leakage reactances vanishes.

These time constants commonly used generator parameters in an industrial context and are discussed in textbooks on electrical machines like the ones by Kundur (1994) and by Krause (2002). The *AI* and *CAI* results in percentage of each stage are shown in Table 2.

**Open-circuit stage:** it was noticed that SMORA gives similar results if the subtransient ($\tau_{d0}''$, $\tau_{q0}''$), and transient ($\tau_{d0}'$) time constant are taken into account or not. This stage runs from $t_0$=0 s to the instant when the switch is turn on at $t_{on}$=30 s. In this scenario, SMORA with a $\beta$=99.5% suggests the elimination of nine elements. Figure 9 presents the reduced model of this scenario. It can be seen that almost all the elements in *d*-axis are gone. This reduction shown that in an open-circuit test the $i_f$, $X_{ad}$, and $\omega_n$ are the responsible of the voltage at terminals. Figure 14 shows the dynamics at the outputs of interest in this stage. It is possible to observe how the terminal voltage is reaching its nominal value while the machine is speeding-up.

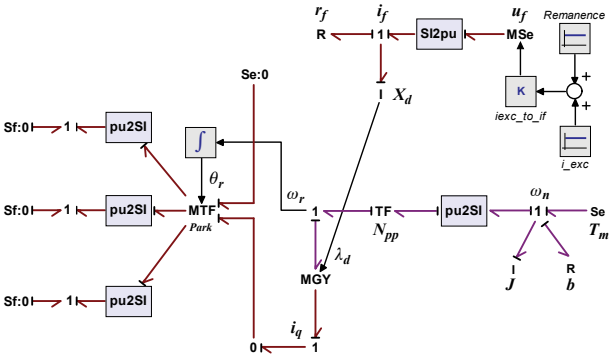


Figure 9: Open-circuit reduced model

**Sudden short-circuit stage:** the subtransient ($\tau_d''$), and transient ($\tau_d'$) time constants have to be taken into account in order to be able to capture the dynamic behavior in a satisfactory manner. The first scenario is the subtransient. It starts at $t_{on}$ =30 s up to $t_d''$= 30.02 s. In this scenario it was seen that a threshold of 93% was sufficient to obtain a satisfactory result. Besides, the mutual inductance of the *q*-axis was maintained rather than the damping winding resistor in *d*-axis. This is justified by the fact that both elements have similar activity. Nevertheless, by maintaining the inductance it is possible to improve the outputs of interest. Figure 10 shows the reduced model.

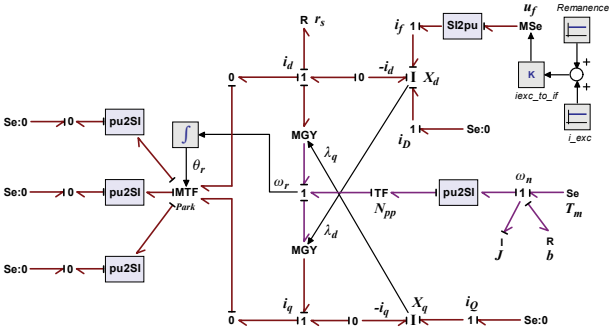


Figure 10: Subtransient short-circuit reduced model

The second scenario is the transient instant. It runs from $t_d''$= 30.02 s to $t_d'$= 30.41 s. In this scenario all the inductances have a high activity, so only one element can be removed. Note that this scenario results in the same model as the one obtained from MORA applied to the whole simulation time. However, in this case the model will be used during a shorter time, since high frequencies due to switching effects have been removed, the model is suitable to use in a fixed-step method. Figure 11 shows the BG model for this scenario.

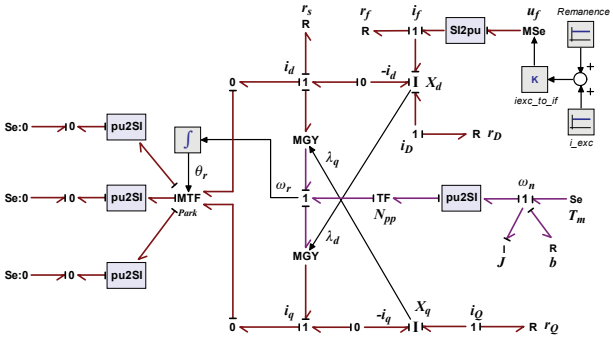


Figure 11: Transient short-circuit reduced model

In the third scenario the short-circuit steady-state runs from $t_d'$= 30.41 s to the moment that the switch is off at $t_{off}$=65 s. It is possible to consider a threshold of 99.99%. Similar to the previous case, the mutual inductance in *q*-axis is chosen instead of the stator resistor on the same axis in order to obtain better accuracy.
Figure 12 presents the short-circuit steady-state reduced BG model.

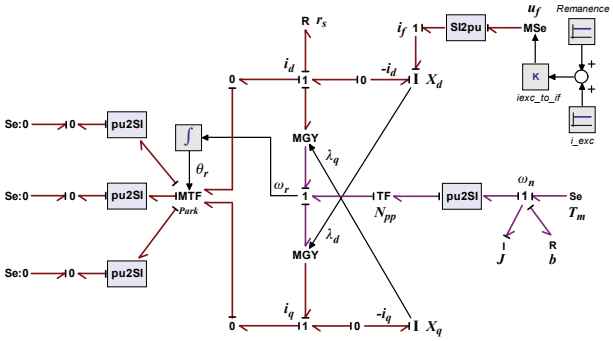


Figure 12: Steady-state short-circuit reduced model

Table 2: Stages element activity indices given by SMORA

| Open-Circuit [0 $t_{on}$] | | | Short-Circuit | | | | | | | | | Open-Circuit [$t_{off}$ $t_f$] | | |
|---|---|---|---|---|---|---|---|---|---|---|---|---|---|---|
| | | | Subtransient [$t_{on}$ $t_d''$] | | | Transient [$t_d''$ $t_d'$] | | | Steady-State [$t_d'$ $t_{off}$] | | | | | |
| **Ele.** | **AI** | **CAI** | **Ele.** | **AI** | **CAI** | **Ele.** | **AI** | **CAI** | **Ele.** | **AI** | **CAI** | **Ele.** | **AI** | **CAI** |
| $r_f$ | 96.07 | 96.07 | $X_{lf}$ | 28.52 | 28.52 | $X_{lf}$ | 40.02 | 40.02 | $r_{sd}$ | 70.94 | 70.94 | $r_f$ | 86.46 | 86.46 |
| $X_{ad}$ | 3.22 | 99.29 | $X_{lsd}$ | 17.66 | 46.19 | $X_{lsd}$ | 20.03 | 60.05 | $r_f$ | 26.81 | 97.76 | $X_{ad}$ | 6.78 | 93.24 |
| $X_{lf}$ | 0.59 | 99.88 | $X_{lQ}$ | 16.61 | 62.80 | $X_{lQ}$ | 10.63 | 70.68 | $X_{lf}$ | 1.58 | 99.33 | $X_{lf}$ | 3.29 | 96.53 |
| $r_D$ | 0.12 | 100 | $X_{lD}$ | 10.35 | 73.15 | $r_{sd}$ | 7.41 | 78.09 | $X_{lsd}$ | 0.61 | 99.95 | $X_{lD}$ | 1.35 | 97.88 |
| $X_{lD}$ | 0.00 | 100 | $X_{lsq}$ | 10.04 | 83.19 | $X_{lsq}$ | 6.40 | 84.49 | $X_{ad}$ | 0.04 | 99.99 | $X_{lsd}$ | 0.58 | 98.46 |
| $r_{sq}$ | 0.00 | 100 | $X_{aq}$ | 3.63 | 86.83 | $X_{lD}$ | 5.30 | 89.79 | $r_{sq}$ | 0.01 | 100 | $r_D$ | 0.57 | 99.04 |
| $X_{lsd}$ | 0.00 | 100 | $r_{sd}$ | 3.55 | 90.37 | $r_f$ | 2.41 | 92.20 | $X_{aq}$ | 0.00 | 100 | $X_{lQ}$ | 0.49 | 99.53 |
| $X_{aq}$ | 0.00 | 100 | $r_D$ | 3.06 | 93.43 | $X_{aq}$ | 2.28 | 94.48 | $X_{lD}$ | 0.00 | 100 | $X_{lsq}$ | 0.30 | 99.82 |
| $r_Q$ | 0.00 | 100 | $X_{ad}$ | 2.35 | 95.78 | $X_{ad}$ | 1.75 | 96.23 | $X_{lsq}$ | 0.00 | 100 | $X_{aq}$ | 0.11 | 99.93 |
| $X_{lsq}$ | 0.00 | 100 | $r_Q$ | 2.29 | 98.07 | $r_Q$ | 1.60 | 97.83 | $X_{lQ}$ | 0.00 | 100 | $r_Q$ | 0.03 | 99.96 |
| $r_{sd}$ | 0.00 | 100 | $r_{sq}$ | 1.30 | 99.37 | $r_D$ | 1.26 | 99.09 | $r_D$ | 0.00 | 100 | $r_{sd}$ | 0.03 | 99.99 |
| $X_{lQ}$ | 0.00 | 100 | $r_f$ | 0.63 | 100 | $r_{sq}$ | 0.91 | 100 | $r_Q$ | 0.00 | 100 | $r_{sq}$ | 0.01 | 100 |

Figure 14 shows the typical curves for this test. There is a large peak at the stator current that contains AC components, and DC components. Those stator DC components interact with the field flux producing a pulsating torque in the shaft. Figure 15 shows a zoom at the moment of short-circuit.

**Sudden open-circuit stage:** It runs from $t_{off}$=65 s until the simulation is over at $t_f$=80 s. Similar to the previous open-circuit test, the time constants are not considered. A threshold of 99% was chosen. The BG model is shown in Figure 13. Figure 16 shows detailed views of the dynamic responses of the outputs of interest that result from the suddenly opened circuit.

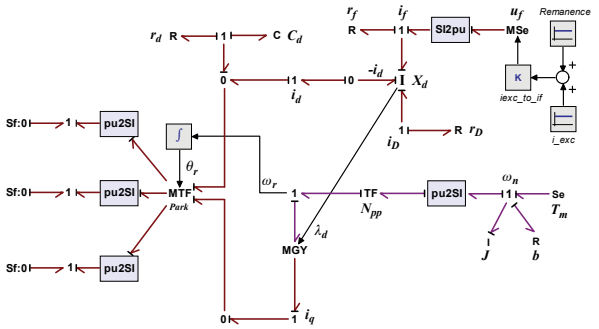


Figure 13: Final open-circuit reduced model

It is important to notice that the *I*-multiport was mathematically manipulated in order to remove its unnecessary ports. The 20-sim® processing of the reduced and original models can be compared in Table 3.

Table 3: 20-sim® processing for original and reduced model

| | Eqs. | Ind. states | No. steps |
|---|---|---|---|
| **Open-Circuit** | 116 | 4 | 101,627 |
| **Subtransient** | 127 | 8 | 208 |
| **Transient** | 130 | 8 | 3,807 |
| **Steady-State** | 119 | 5 | 166,213 |
| **Open-Circuit** | 124 | 7 | 68,581 |
| *Total* | | | 340,436 |
| **Original model** | 160 | 13 | 2,754,759 |

It can be seen from the information in Table 3 that the total number of steps done by the integration method (Vode-Adams) was reduced to 87% compared to the original model.

The number of equations in each stage was reduced in average 23% compared with the original model equations. Moreover, the number of independent states in each stage decreased in a range from 46% - 70% compared with the original model.

This iterative application of MORA in SMORA gives good results in the reduction. This can be confirmed also by the analysis of the fit of the reduced model with the original model. Equation (11) gives a fit of 93% for the voltage at *phase-a*; for the current at *phase-a* is 90%; for the torque in the shaft is 88%; finally, for the current in the field is 97%. Figure 14 shows the comparison between the outputs of interest of the original and the reduced model.

## CONCLUSIONS

This paper describes a model order reduction algorithm called SMORA, i.e. Switched MORA. MORA was previously developed by Loucas et al. (1997).

It was shown that the original MORA has limitations when it is applied to systems which contain sudden transitions, e.g. due to switches, as shown in the example of a sudden short-circuit test applied to a SG. The proposed SMORA separately considers the different stages of the generator by reducing the time window where MORA is applied to each stage.

By concentrating on one stage at the time with a particular behavior the corresponding dynamics effects are described by the reduced model for that stage in a more accurate manner. These stages or time spans are distinguished by means of switching events and time constants of the SG. The reduced models need to be simulated in series in order to obtain the full behavior of the system. On top of that, the reduced models are now suitable to be used with a fix-step method.

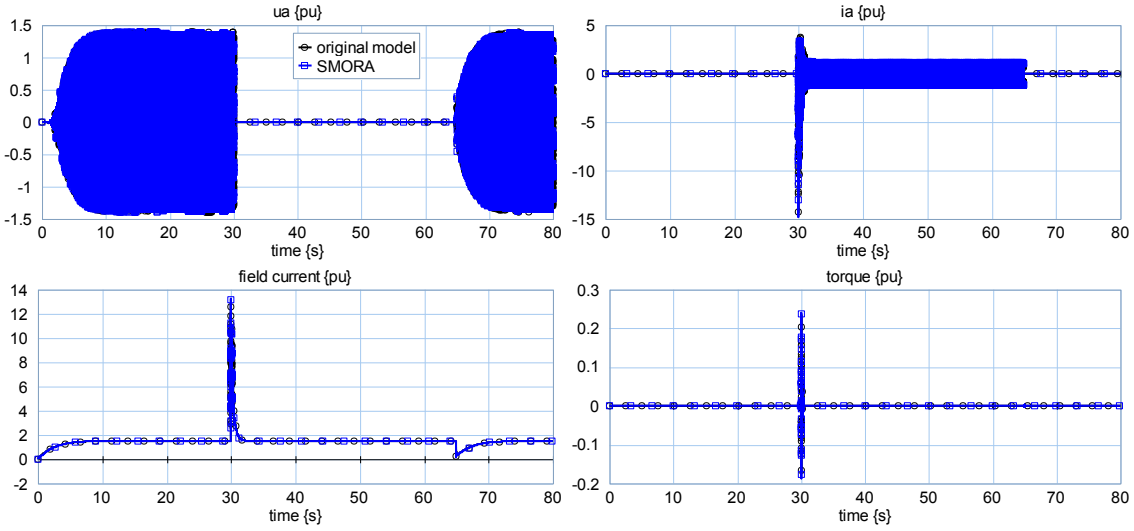


Figure 14: Outputs of interest comparison between original model and reduced model (SMORA) at open-circuit stage [0 30] seconds, sudden short-circuit stage [30 65] seconds, and sudden open-circuit [65 80] seconds

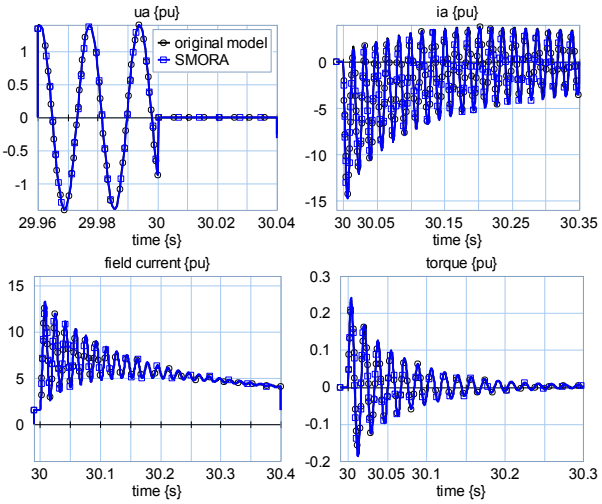

Figure 15: Zoom at sudden short-circuit on Figure 14

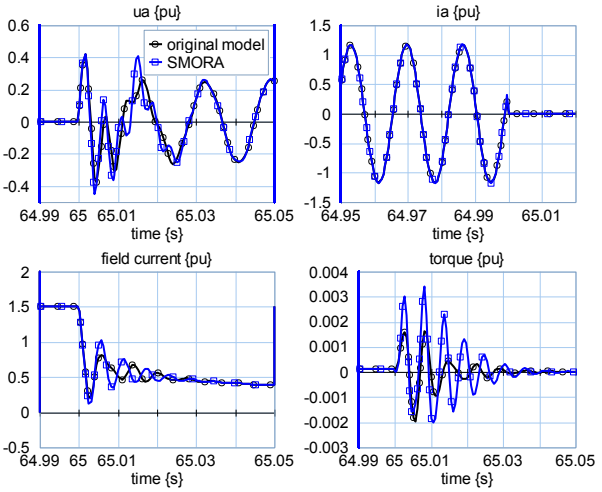

Figure 16: Zoom at sudden open-circuit on Figure 14

The results of this modification show that the correspondence between the original response and the reduced one is high. At the same time, the total number of computational steps of the reduced models was decreased up to 87% of the original model.

So far, SMORA presents only theoretical results. The main lines for future work include to implement SMORA in a real HIL simulator and in a multidomain system.

Moreover, SMORA appears a promising technique since the reduced models per scenario may be reusable. If for example the modeler has a collection of reduced models of various scenarios, it is possible to exchange the succession of the scenarios in order to create new tests.

The experience of the modeler still plays a role in the decision of keeping or eliminating certain elements. Further automation of this process remains a topic of future research.

## ACKNOWLEDGMENTS

The authors wish to thank CONACYT (Mexican National Council of Science and Technology) and SEP (Mexican Secretary of Public Education) for the funding of this research.

## REFERENCES

Anderson, P.M.; and Fouad, A.A. 2003. *Power System Control and Stability*. 2nd edition, John Wiley & Sons, USA.

Borutzky, Wolfgang (Ed.). 2010. *Bond Graphs: A Methodology for Modelling Multidisciplinary Dynamic Systems*, Springer, London.

Breedveld, P.C., 1985. "Multibond graph elements in physical systems theory". *Journal of the Franklin Institute*, Vol. 319, Issues 1-2, (Feb.), Pages 1-36, ISSN 0016-0032

Breedveld, P.C., 1996. "The context-dependent trade-off between conceptual and computational complexity illustrated by modelling and simulation of colloding objects", proceedings IEEE-SMC CESA'96 conference, Lille, 48-54.

Corzine, K.A.; Kuhn, B.T.; Sudhoff, S.D.; and Hegner, H.J. 1998. "An improved method for incorporating magnetic saturation in the q-d synchronous machine model". *Energy Conversion*, *IEEE Transactions*, vol.13, no.3 (Sept.)

Hanselmann, H. 1996. "Hardware in the loop simulation testing and its integration into a CACSD toolset". *Proc. IEEE Int. Symp. Comput.-Aided Control Syst. Des.*, Dearborn, MI, (Sep.), 152-155.

IEEE Std 1110-2002. *IEEE Guide for Synchronous Generator Modeling Practices and Applications in Power System Stability Analyses*, IEEE Power Engineering Society, New York, (Nov).

Junco, S.; Diéguez, G.; Ramírez, F. 2007. "On commutation modeling in Bond Graphs". *Proc. Int. Conf. on Bond Graph Modeling and Simulation*, San Diego, 12-19.

Karnopp, D.C.; Margolis, D.L.; and Rosenberg, R.C. 1990. *System Dynamics: A Unified Approach*. John Wiley & Sons, Inc., New York, USA.

Krause, P.C.; Wasynczuk, O.; and Sudhoff, S.D. 2002. *Analysis of Electric Machinery and Drive Systems*, 2nd edition, John Wiley & Sons, Inc. Publication, New York, USA.

Kundur, Prabha. 1994. *Power System Stability and Control*. Mc-GrawHill, California, USA.

Ledin, J. 1999. "Hardware in the loop simulation" *Embedded System Programming*, Vol. 12, No. 2, (Feb.), 42-60.

Louca, L.S.; Stein, J.L.; Hulbert, G.M.; and Sprague, J. 1997, "Proper Model Generation: An Energy-Based Methodology". *Proceedings of the International Conference on Bond Graph Modeling ICGBM '97*, Society for Computer Simulation, San Diego, CA.

Park, R.H. 1929. "Two-Reaction Theory of Synchronous Machines-Generalized Method of Analysis". *Part I AIEE Transactions*, Vol. 48 (July), 716-727.

Paynter, H.M. 1961. *Analysis and Design of Engineering Systems*, The M.I.T. Press, Cambridge, Massachusetts.

Rankin, A.W. 1945. "Per-Unit Impedances of Synchronous Machines". *Transactions of the American Institute of Electrical Engineers*, vol.64, no.8 (Aug.), 569-573.

Sahm, D. 1979. "A Two-Axis, Bond Graph Model of the Dynamics of Synchronous Electrical Machines", *Journal of the Franklin Institute*, vol. 308, No. 3, 205-218.

## APPENDIX A: SYNCHRONOUS MACHINE PARAMETERS

$S_n = 4100\,kVA$, $PF = 0.9$, $V_{nL} = 6.6\,kV$, $I_n = 358.7\,A$,

$\omega_m = 720\,\mathrm{r/min}$, $J = 1100\,kgm^2$, $X_d = 1.32\,pu$,

$X_d' = 0.222\,pu$, $X_d'' = 0.16\,pu$, $X_q = 0.66\,pu$,

$X_q'' = 0.159\,pu$, $\tau_{d0}' = 2.45\,s$, $\tau_d' = 0.41\,s$, $\tau_d'' = 0.02\,s$,

$\tau_{d0}'' = 0.03062\,s$, $\tau_{q0}'' = 0.16604\,s$, $\tau_q = 0.04\,s$